[Frontiers in Bioscience 12, 3601-3616, May 1, 2007]

The biologic basis of *in vivo* angiogenesis imaging

Iclal Ocak[1], Peter Baluk[2], Tristan Barrett[1], Donald M. McDonald[2], Peter Choyke[1]

[1]Molecular Imaging Program, National Institutes of Health, Bethesda, Maryland, USA, [2]Comprehensive Cancer Center, Cardiovascular Research Institute, and Department of Anatomy, University of California, San Francisco, California, USA

TABLE OF CONTENTS

1. ABSTRACT

Knowledge of the different physiology and endothelial markers present in tumor vessels is essential to enable both the development of new anti-angiogenic chemotherapeutic agents and of more specific imaging techniques. Tumor blood vessels are disorganized, irregular in caliber, tortuous, and do not have specialized features of normal arterioles, capillaries or venules. Neo-angiogenic tumor vessels have large gaps between or through cells, loose pericytes, and discontinuities or redundant layers within the basement membrane, rendering these vessels hyper-permeable. Furthermore, the endothelia of tumor vessels may express unique markers on their surface. Imaging is becoming increasingly important in the evaluation of angiogenesis. Clinical imaging is minimally invasive and enables sampling of the whole tumor in a nondestructive manner. The patterns of increased permeability seen on Dynamic contrast-enhanced Magnetic Resonance Imaging (DCE-MRI) mirror the known ultrastructural defects associated with angiogenic vessels. Conventional low-molecular weight contrast agents are currently in clinical use for DCE-MRI studies and have proven successful in detecting changes related to novel angiogenic inhibitors. However, they are relatively non-specific. Macromolecular contrast media may be more suitable for imaging tumor vessels. It is hoped that imaging modalities can be adapted to specifically target markers expressed on the endothelium of tumor vessels. The number of cell surface markers of angiogenesis is relatively low, and only small amounts of contrast agents can bind to these receptors; currently only Positron Emission Tomography (PET) and Single Photon Emission Computed Tomography (SPECT) tracers have sufficient sensitivity to allow detection at this low level. Despite limitations in their spatial resolution, PET and SPECT imaging are more likely to enter the clinic as targeted angiogenesis imaging methods. The quest for selective targets on the tumor vasculature continues, currently the integrin family of receptors offer the most promise but other targets are being pursued by investigators. Serial analysis of gene expression or *in vivo* phage display may help identify new, more selective, markers that can be utilized for the targeted imaging and treatment of angiogenesis.

2. INTRODUCTION

Tumors sustain their growth and expansion by recruiting new blood vessels *via* angiogenic sprouting of existing vessels. Most tumors have a rich vasculature, but the blood vessels are highly abnormal and the vascular network is chaotic and dysfunctional. As a result, blood vessels in tumors differ from those in normal organs, in some cases having an increased blood volume and leakiness - expressed in clinical imaging as the vascular permeability/surface area product (PS). Angiogenesis inhibitors are designed to exploit these differences, with the goal of eliminating tumor vessels without destroying the normal vasculature.

The molecular diagnosis of angiogenesis relies on the identification of particular markers specific to the endothelium of angiogenic vessels. Angiogenic vessels can be identified by immunohistochemical staining using

antibodies to CD31, VEGFR-2, CD105 and other markers of endothelial cells. The classic method of assessing angiogenesis is to measure the microvascular density by staining for endothelial cells using the marker CD31. By simultaneously staining for multiple molecular markers of angiogenesis at the cell and cellular organelle level, it is possible to localize angiogenic vessels. However, many normal blood vessels also express these markers and histological methods are based on fixed tissues, are inherently invasive, do not provide information about the real-time physiologic state of the microvasculature, and do not permit monitoring of dynamic cellular processes *in vivo*.

Clinical imaging, which is minimally invasive and safer than repeated biopsies, is an attractive approach for following tumor response to therapy in humans. Contemporary clinical imaging methods include computed tomography (CT), magnetic resonance imaging (MRI), positron emission tomography (PET), single photon emission computed tomography (SPECT), ultrasound (US), and optical imaging. Clinical imaging is able to exploit the morphologic and physiologic differences between normal and neo-angiogenic vessels in tumors, thus permitting a non-destructive assessment of tumor vascularity. Furthermore, contrast agents targeted to endothelial markers of angiogenesis have been developed for imaging modalities with sufficient sensitivity to allow clinical detection of molecular markers of angiogenesis *in vivo*. Progress in this direction has been made primarily in PET, SPECT, and MRI imaging.

Early biomarkers of clinical outcome in response to angiogenic inhibitors are being sought in drug trials since these drugs are often very expensive and early biomarkers may make it possible to show that the therapy is failing long before tumor progression can be measured. Since it is widely understood that these therapies may be cytostatic rather than cytotoxic such early biomarkers become useful indicators of success or failure since they are not based on anatomic changes within the tumor. This is particularly true during the early phases of drug development where the greatest savings can be realized. Both drug developers and clinicians alike use imaging to determine if a drug "hits the target" soon after administration to the patient. Of course, a far more difficult determination is whether the drug is successful in prolonging the survival of the patient. The process by which an imaging "biomarker" becomes a "surrogate" marker - *i.e.* one that predicts patient outcome - is long and requires much validation, but is the ultimate goal of the imaging studies described here.

Angiogenesis imaging techniques fall into two broad categories: those exploiting the abnormal physiology of the neo-angiogenic tumor vessels and those targeting specific endothelial markers of angiogenesis. Dynamic Contrast Enhanced-MRI (DCE-MRI) has recently emerged as the most widespread method for both diagnosis and follow-up of cancers during anti-angiogenic therapies (1-4). Molecularly targeted imaging techniques such as PET and SPECT are being developed to provide *in vivo* molecular characterization of the microvasculature.

Herein, we review the abnormalities of tumor blood vessels that can be exploited by clinical imaging techniques and the expression of molecules on components of tumor vessels that make it possible to target imaging agents to tumor vasculature. With this background, we then focus on functional studies of the microvasculature, exemplified by DCE-MRI, and targeted molecular studies of the microvasculature, exemplified by integrin targeted PET scans.

3. ABNORMALITIES OF TUMOR BLOOD VESSELS

Normal blood vessels are lined by a well-constructed monolayer of tightly joined endothelial cells (Figures 1A-B). The barrier function of the endothelium limits vascular permeability and transendothelial flux of macromolecules. Pericytes or smooth muscle cells are tightly apposed to the abluminal (basal) surface of endothelial cells, and both cell types are enveloped by the basement membrane. The luminal surface of the normal endothelium is usually smooth, and adjacent cells are joined tightly together (Figure 1B). Endothelial cells rarely sprout or divide because most normal blood vessels are quiescent.

Blood vessels of the normal microcirculation are organized in a hierarchy of arterioles, capillaries, and venules, each having distinctive structural and functional characteristics. The microcirculation has many organ-specific specializations, but hierarchical organization is a consistent feature of the microvasculature of all normal organs. In tumors, blood vessels are abnormal in multiple respects. Tumor vessels do not have specialized features of normal arterioles, capillaries or venules and lack hierarchy. Instead, tumor vessels are disorganized, irregular in caliber, tortuous, and have a bizarre branching pattern (5). All components of the wall of tumor vessels are abnormal. Endothelial cells may overlap one another, form multiple layers, and have cytoplasmic processes that project into or across the vascular lumen (Figures 1C-D) (6). Endothelial cells of tumor vessels do not have normal intercellular junctions. Gaps between or through cells (Figure 1E) render tumor vessels leaky to plasma and prone to hemorrhage (6). Extravasated plasma leads to fibrin deposits (7). Endothelial cells of some tumor blood vessels have clusters of fenestrations that are 80-nm in diameter (Figure 1F), but these are not unique to tumor vessels. Endothelial fenestrations can be found in normal organs in the presence of high levels of vascular endothelial growth factor (VEGF) (8). Inhibition of VEGF signaling reduces endothelial fenestrations both in tumors and in normal organs (8). Furthermore, tumor vessels are dynamic. They grow, regress, and constantly change. Blood flow in individual vessels may change directions. Consistent with their dynamic nature, tumor vessels have abundant endothelial sprouts. In tumors, sprouts have a haphazard distribution over the abluminal surface of endothelial cells,

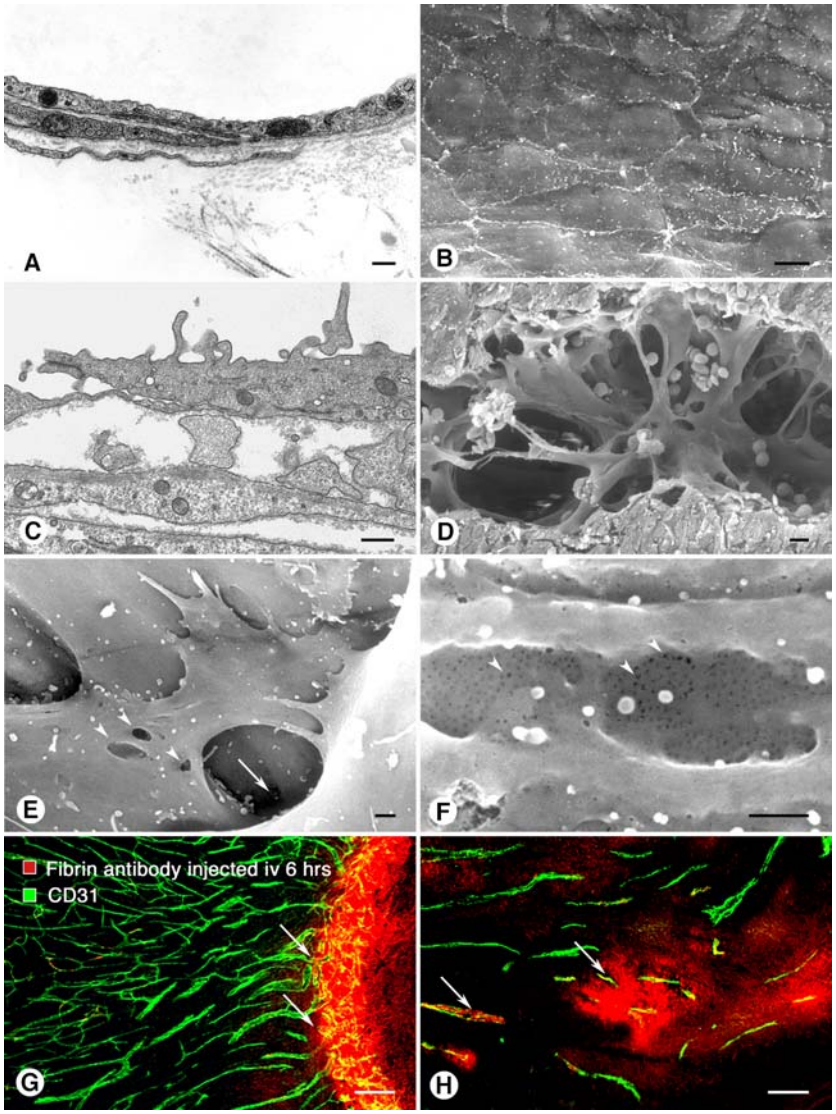

Figure 1. A. Transmission electron micrograph (EM) of normal blood vessel in mouse trachea. The endothelial cell has a relatively smooth surface. Pericyte processes and basement membrane are closely apposed to the endothelial cells. Bar: 2 µm. Reproduced with permission from (79). B. Scanning EM of luminal surface of endothelial cells in a large venule of normal mouse mammary gland. Endothelial cells are relatively flat and smooth and have little overlap and no gaps at their borders. Bar: 5 µm. Reproduced with permission from (6). C. Transmission EM showing abnormalities of blood vessel in mouse MCa-IV breast carcinoma. Endothelial cells range from abnormally thin to abnormally thick with irregular projections into the vascular lumen. Multiple overlapping pericytes with accompanying basement membrane are loosely associated with the endothelium. Bar: 1 µm. Reproduced with permission from (6). D. Scanning EM of endothelial cells in severely abnormal blood vessel in mouse MCa-IV breast carcinoma. The endothelial cells have bizarre shapes and do not form a monolayer but instead project into or across the lumen where they can obstruct blood flow. Bar: 5 µm. Reproduced with permission from (6). E. Higher magnification scanning EM view of endothelial cells in blood vessel in mouse MCa-IV breast carcinoma showing holes that are potential routes for leakage through endothelial cells (arrowheads) and between endothelial cells (arrow). Bar: 1 µm. Reproduced with permission from (6). F. High magnification scanning EM view of blood vessel in mouse MCa-IV breast carcinoma. Collections of 80-nm fenestrae (arrowheads) are located in some regions of the endothelium. Bar: 1 µm. Reproduced with permission from (6). G. Confocal microscopic image of blood vessels (green, stained for CD31) in untreated Lewis lung carcinoma grown subcutaneously in a mouse. Anti-fibrin antibody was injected intravenously 6 hours before sacrifice to stain fibrin deposits (red) and localize sites of plasma leakage. Most staining was in a band at the perimeter of the tumor (arrows). Bar: 200 µm. Reproduced with permission from (7). H. Confocal microscopic image of blood vessels (green, stained for CD31) in Lewis lung carcinoma grown subcutaneously in a mouse, then treated with a small molecule inhibitor of VEGF receptor tyrosine kinases. After treatment, regions of fibrin (red) stained by extravasated anti-fibrin antibody are more abundant around vessels within the tumor (arrows). Bar: 200 µm. Reproduced with permission from (7).

and are not restricted to their usual location at the tips of growing vessels.

As with the endothelial cells of tumor vessels, the pericytes and basement membranes that surround the endothelium are also abnormal. Pericytes are loosely associated with endothelial cells (9), and functional relationships between the two types of cells are disturbed (10). Basement membrane, which is made by and envelops endothelial cells and pericytes, may be abnormal in thickness and have discontinuities, redundant layers, and an abnormal composition. Abnormal matrix molecules such as the oncofetal form of fibronectin with an extra-domain B (ED-B) and metalloproteinases may be present (11, 12). Beyond the abnormal vasculature, the tumor stroma contains activated fibroblasts, myofibroblasts, macrophages, or other immune cells (13, 14). It has been demonstrated that in implanted tumors in preclinical models (Figure 1G), and in some human tumors, that blood vessels are especially abundant, dynamic, chaotic, and leaky at the perimeter, unlike the more sparse vasculature in the interior where regions of necrosis are common (7). However, tumor vessels regardless of their location do not become 'established' in the sense of the stable vasculature of normal organs. Their abnormalities persist, but the severity of the defects may vary from region to region within a tumor, from tumor to tumor, and with the growth rate and aggressiveness of the tumor.

One of the consequences of the structural defects in the endothelium of tumor vessels is the potential for increased leakage of plasma, both in relation to the amount of extravasation and to size of substances that cross the endothelium. The obvious gaps and holes observed in the endothelial cell barrier offer a route for increased leakiness of tumor vessels. Macromolecules and particles that do not extravasate from most normal blood vessels can leak from tumor vessels (15). Physical gaps between endothelial cells and holes through the cells serve as points of extravasation and explain the increased leakiness (6). However, endothelial permeability does not alone determine the magnitude of transendothelial leakage or flux from blood vessels, and other pathways may also contribute (16). The amount of leakage is governed not only by the physical porosity of the barrier but also by vascular surface area and the balance of hydrostatic and osmotic driving forces across the barrier, as formally defined by the Starling equation (17) which, in turn, is related to the capacity of the peritumoral lymphatics to drain excess fluid from the tumor periphery.

Most tumors have *less* blood flow than would be expected based on their vascularity because the tumor vasculature is relatively inefficient as a delivery system for oxygen and nutrients. As a consequence, regions of tissue hypoxia or necrosis are common despite apparently excessive amounts of microvasculature. Also, despite the abnormal leakiness of tumor vessels, convective transport of macromolecules to tumor cells is impaired. High interstitial pressure, which results in part from the relative insufficiency of functional lymphatic vessels for drainage of extravasated fluid, reduces the hydraulic driving force for extravasation and thus the transendothelial flux of molecules that move by convection (18, 19). Interstitial pressure becomes progressively greater toward the tumor center. An important challenge is to reconcile preclinical and clinical estimates of endothelial barrier function and transendothelial and intratumoral transport of macromolecules (20, 21) and will require the coordinated measurements of vascularity and interstitial pressure in human tumors (20, 22).

The dynamic nature and growth factor-dependency of tumor vessels can be exploited by angiogenesis inhibitors, which not only interfere with tumor vessel growth, but also cause regression of a significant proportion of the vasculature in some tumors. Second, the abnormal leakiness of tumor vessels can be exploited to selectively expose tumor parenchyma to large molecules such as viral or liposomal therapeutic vectors that do not cross the normal endothelium. This abnormal 'leakiness' of tumor vessels can also be exploited by clinical imaging to locate and follow the size of primary tumors or metastases. It is hypothesized that if the abnormal tumor blood vessels can be therapeutically 'normalized', then the delivery of other therapeutic agents to the tumor can be improved (20). Inhibitors of VEGF signaling and other angiogenesis inhibitors tend to correct the structural and functional abnormalities of tumor vessels that survive treatment (8, 20). Although overall tumor vascularity decreases, surviving tumor vessels are less leaky and have increased conductance, and lower interstitial pressure (20, 22). Such normalization leads to increased local blood flow and improved delivery of macromolecules to tumor cells (Figure 1H) within a critical distance from normalized tumor vessels (20). Improved blood flow will also reduce regions of hypoxia, low glucose and acidosis that are common in tumors, rendering tumor cells around normalized tumor vessels more susceptible to radiotherapy (22). In the next section we consider an *in vivo* imaging modality that relies on vascular permeability-surface area.

4. DYNAMIC CONTRAST ENHANCED-MRI (DCE-MRI)

DCE-MRI provides both detailed morphological and functional information about tumor microcirculation in the same study. DCE-MRI can also monitor the effects of anti-angiogenic therapies without requiring exposure to ionizing radiation. DCE-MRI studies provide estimates of vascular permeability/surface area product (PS) and extravascular volume (v_e) by measuring the leakage rate of low molecular weight MR contrast agents into tumors. This method has emerged as a useful technique for noninvasive imaging of tumor vasculature in preclinical and clinical models. The underlying basis for the success of DCE-MRI can be readily understood from the structural abnormalities in the integrity of the endothelial surface of angiogenic blood vessels.

4.1. DCE-MRI acquisition design

DCE-MRI is the rapid acquisition of serial MR images before, during, and after the bolus injection of an

intravenous gadolinium-based contrast agent. Low molecular-weight (LMCM) or macromolecular-weight contrast molecules (MMCM) can be used for DCE-MRI. The majority of DCE-MRI studies performed clinically rely on FDA approved LMCMs. Gadolinium-chelates are used for such studies (at a usual dose of 0.1 mmol/kg), and are typically administered by means of a mechanical injector to ensure rapid and consistent injections. In order to obtain valid estimates of tumor response, it is important that the same region of tumor is imaged in the same way on each patient visit. For this reason, the target lesion(s) need to be pre-selected and three-dimensional (3D) protocols, which provide data over the whole tumor, are preferred. Dedicated receive-only-coils, and breath-hold techniques, when needed, are used to maximize signal to noise ratios and minimize body motion artifacts. A typical dynamic scan consists of three dimensional (3D) spoiled gradient echo images after the intravenous injection of a low molecular weight Gadolinium chelate, allowing image acquisition within a reasonable time-span (*i.e.* 5-15 seconds per 3D data set). Baseline T1 and T2 weighted MRIs are also obtained to provide detailed anatomic depiction of the tumor, whilst the dynamic scans provide functional information about the response of the microvasculature to therapy (23).

4.2. DCE-MRI ANALYSIS

Pharmacokinetic quantitative analysis of DCE-MRI is the method by which vessel permeability changes are measured. DCE-MRI data is typically analyzed with a variant of a two compartment pharmacokinetic model and the archetype of these models is the "Tofts' two-compartment kinetic model" (24). In this two compartmental model, an injected contrast agent leaks into the extravascular, extracellular space (EES) at a rate predicted by the vessel's permeability and surface area. Angiogenic vessels would be expected to be very leaky and thus have a rapid forward leakage rate. The contrast agent then leaks back from the EES to the vascular space at another rate constant which is also increased in tumor vessels (3, 24-28). In order to quantitate these rate constants, the "arterial input function" is usually measured. This is obtained by measuring the signal from an artery in the vicinity of the tumor. Inclusion of the input function compensates for changes related to the rate of injection and the cardiac status of the patient.

In addition to the arterial input function, the tissue T1 must be determined. This is needed because the relation between the tissue Gadolinium concentration and the change in signal intensity is dependent upon the baseline T1 of the tissue. This is unlike CT in which there is a fixed relationship between iodine concentration and Hounsfield units (the unit of CT density), regardless of the baseline attenuation. Thus, it is necessary to obtain a "T1 map" prior to injection. This allows the conversion of MR signal intensity into Gadolinium concentration. T1 maps are typically created by imaging the tissue prior to contrast agent administration with varying repetition times of the initial pulse sequence or varying flip angle.

Once the arterial input function and the T1 of the tissue are determined, the two compartment model can be used to fit the time signal data to curves whose parameters are h the rate constants of the two compartment model which include K^{trans} (forward flow rate; a combination of flow and PS), k_{ep} (backflow rate), Ve (volume of the extracellular, extravascular space), and FpV (fraction of plasma volume). Another parameter which is helpful is the "area under the gadolinium concentration curve" (AUGC) which provides an index of the total leakage of contrast media within the tumor over a fixed time. Early after anti-angiogenic therapy these quantitative DCE-MRI parameters decrease dramatically. This is likely due to reductions in vascular PS and pruning of vessels resulting in lower blood flow.

4.3. DCE-MRI in drug trials - preclinical experiences

Quantitative DCE-MRI with LMCMs was initially tested in pre-clinical drug trials involving tumor models. Typical of these experiments is Marzola *et al* who investigated the anti-angiogenic effect of SU6668, an oral small molecule, inhibitor of the receptor tyrosine kinases (RTK): vascular endothelial growth factor receptor 2 (Flk-1/KDR), platelet-derived growth factor receptor, and fibroblast growth factor receptor 1, in a HT29 human colon carcinoma xenograft model using DCE-MRI (29). They showed a 51% (tumor rim) and 26% (core) decrease in the average vessel PS after only 24 hours of treatment, with a 60% tumor growth inhibition after 14 days. Interestingly, the rim of the tumor, which is generally more angiogenic, experienced the greatest decrease in vascularity. In another example, Lee *et al* investigated the use of PTK/ZK, an oral angiogenesis inhibitor that specifically targets all VEGF receptor tyrosine kinases (30). They used a mouse model of metastatic melanoma and employed DCE-MRI on day 0 (baseline) and day 3; reductions in the AUGC were seen by day 3. In another study, Lussanet *et al*, evaluated DCE-MRI in a mouse melanoma model after the use of the angiostatic compound Anginex, which is thought to disrupt endothelial cell membranes, and TNP-470, which selectively inhibits DNA synthesis in endothelial cells. Studies on day 16 showed a 44% decrease in the K^{trans} value of the tumors in mice treated with TNP-470 and a 64% decrease in K^{trans} in Anginex-treated mice as compared with controls (31). Thus, a variety of pre-clinical experiments support the role of DCE-MRI in angiogenic inhibitory therapy.

4.4. DCE-MRI in drug trials - clinical experience

DCE-MRI has been used extensively in Phase I and II clinical trials of angiogenic inhibitors (Figures 2A-E). PTK787/ZK 222584 (PTK/ZK), a VEGF RTK antagonist has been evaluated with DCE-MRI. Patients with advanced colorectal cancer and liver metastases demonstrated significant reductions in tumor PS and vascularity within 2 days of administration of the drug (30, 32). Another agent, AG-013736, selectively inhibits the tyrosine kinase activities of all known VEGF receptors and platelet-derived growth factor receptor-ß. Liu *et al* performed DCE-MRI to evaluate response to AG-013736 in 36 patients with advanced solid tumors (33). DCE-MRI

Table 1. Comparison of low molecular weight DCE-MRI anti-angiogenesis drug trials[1]

Drug	Authors	Patient population	DCE-MRI parameters measured	Time points	Results
PTK/ZK	Morgan *et al* (32)	Advanced colorectal cancer with liver metastasis	AUGC, Ki, C_{max}, C_{min}	Day 0, 2, 28	Mean reduction of Ki of 43% at d2. Degree of reduction predicts disease progression
PTK/ZK	Lee *et al* (30)	Colorectal carcinoma with liver metastases	Ki, AUGC	Day 0, 2, 28, 56	Reduction in AUGC to 47% of baseline
PTK/ZK	Mross *et al* (80)	Breast or colorectal carcinoma with liver metastasis	AUGC, Ki	Day 0, 28	Significant reduction of Ki at d2 at doses >750 mg, still present at d28
PTK/ZK	Thomas *et al* (81)	Advanced solid tumors	Ki, AUGC	Day 0, 2, 28	>40 % reduction in Ki at day 2 predicted non-progression
Combretastatin A4 phosphate	Galbraith *et al* (82)	Advanced solid tumors	K^{trans}, k_{ep}, V_e, AUGC	Day 0, 4 hours, 24 hours	Significant reduction in K^{trans} of 37% (4 hrs) and 29% (24 hrs) in higher dose group. Normal muscle and kidney unaffected
AG-013736	Liu *et al* (33)	Advanced solid tumors	AUGC, K^{trans}	Day 0, 2, 28, 56	>50% reduction in AUGC and K^{trans} at d2, persisted at d28 of treatment
Bevacizumab	Wedam *et al* (34)	Locally advanced breast cancer	K^{trans}, k_{ep}, FpV, V_e	Day 0, after cycles 1, 4 and 7 of treatment	Reduction in K^{trans} (34.4%), K_{ep} (15%) and V_e (14.3%) post bevacizumab
SU6668	Xiong *et al* (35)	Advanced solid tumors	AUGC, Maximum slope	Day 0, 28, 84	2 of 4 patients had significant reductions in AUGC and/or max slope
SU5416	Medved *et al* (38)	Metastatic colon cancer, melanoma, or locally advanced mesothelioma	C_{max}, AUGC	Day 0, 56	AUGC (90s) reduced -0.84 minute kg/liter (P=0.05). Normal liver unaffected

[1]See text for definitions of AUGC, K^{trans}, K_{ep}, FpV, V_e. Ki measurement is equivalent to K^{trans}. C_{max} = maximum plasma concentration, C_{min} = minimum plasma concentration.

showed a >50% decrease in K^{trans} and AUGC measurements as early as two days after starting therapy, with changes persisting after four weeks. Wedam *et al* (34) recently demonstrated a reduction in K^{trans}, k_{ep} and Ve values for patients with locally invasive breast cancer, following treatment with bevacizumab, a recombinant humanized monoclonal antibody to VEGF (29, 35-37). Medved *et al* showed significant reductions in AUGC and maximum contrast concentration for tumors treated with SU5416, however, normal liver remained unaffected by this medication (38).

Thus, quantitative DCE-MRI is being used in clinical trials and is yielding promising results for monitoring early tumor response to anti-angiogenic agents. These preliminary studies also suggest that DCE-MRI may be able to predict the optimal dosing of a selected drug in Phase I trials, whilst showing efficacy at time points as early as two days, which correlated to, and predicted, clinical response. Table 1.

4.5. Validation and limitations of DCE-MRI

LMCM Gadolinium-based DCE-MRI has been evaluated widely in last decade. Typically, the effect of the drug must be large in order to overcome variations caused by the image acquisition process, inter-patient differences and motion artifacts (Figures 2C-E), but in most cases this condition is satisfied. Generally, it is felt that the effect of the drug must be >40% in order to be clearly recognized with DCE-MRI, any smaller changes may be simply due to the MRI technique which has a coefficient of variation of approximately 10-20%. Another limitation of DCE-MRI with low-molecular contrast agents is that it is non-specific and will enhance both benign and malignant tissues (39). Further, due to limited fields of view, only one, or at most a cluster of tumors can be evaluated in a single session leading to potential sampling biases. DCE-MRI is still not widely available, not because hospitals lack the equipment, but because of the lack of standardized acquisition methods and analytic software as well as the lack of reimbursement. Standardized methods of DCE-MRI acquisition and analysis are essential in order for this method to become a standard method of monitoring drug response.

4.6. Macromolecular contrast agents in DCE-MRI

Because angiogenic vessels are characterized by large pores or fenestra in the endothelial lumen, macromolecular contrast media are well suited to DCE-MRI. MMCMs range in molecular weight from 5 kDa-90 kDa (*cf* Gd-DTPA at ~ 600 Da). Their large molecular diameters lead to prolonged intravascular retention and they leak more slowly through normal endothelium, which may make them more selective for the tumor neo-vasculature than LMCMs. Thus, K^{trans} values obtained with MMCM, whilst lower, may more accurately reflect PS for molecules of a larger diameter and therefore be more selective for angiogenic vessels within tumors. Typically MMCMs employ either Gd or iron compounds to produce an MR signal. Examples of MMCMs include ultrasmall paramagnetic iron oxides, dendrimers (Figure 2F), viral particles and liposomes. These agents are still at an experimental stage and only a limited number are undergoing clinical testing.

Because MMCMs are potentially more selective for tumor blood vessels they are also being considered as drug delivery platforms. For instance, it may be possible to embed drugs within the matrix of the MMCM and have them accumulate preferentially at tumor sites because of enhanced permeability and retention (EPR). In the case of particles with a solid iron core, it may be possible to heat those particles externally causing the drug to be released from the particle thus delivering high local concentrations of the drug.

5. MOLECULAR TARGETED IMAGING

Whilst DCE-MRI provides functional

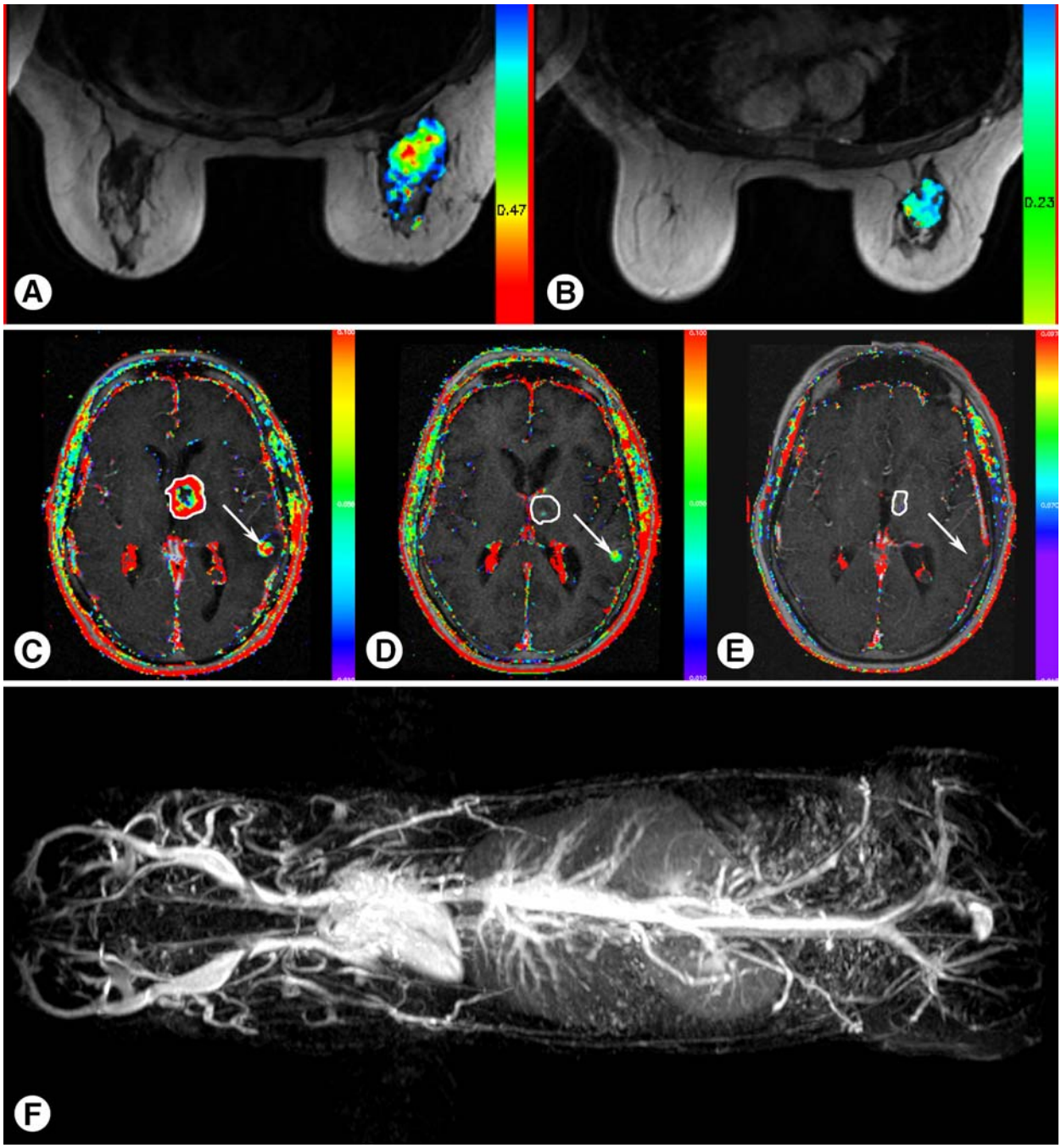

Figure 2. A-B. Gd-DTPA DCE-MRI derived K^{trans} maps in a patient diagnosed with breast cancer. Phase II trial of an anti-VEGF mAb treatment, images taken (A) before and (B) after 1 cycle (4 weeks) of treatment. Scans show a decreased size of tumor as well as leakiness of the vessels. C-E. Gd-DTPA DCE-MRI derived K^{trans} permeability maps in a patient diagnosed with glioblastoma multiforme. (C) Baseline image, before treatment with anti-VEGF mAb, (D) 4 weeks and (E) 7 months post treatment. There is resolution of main lesion (circled) and the satellite metastasis (arrow) due to decreases in permeability caused by the antibody. F. Macromolecular contrast agent DCE-MRI in an experimental model. Dendrimer based agent containing Gadolinium ions in a 'TUBO' mouse model, showing 'blood pool' retention of contrast within the vascular system 30 minutes post injection.

information, it cannot discern molecular markers of tumor angiogenesis. Because inhibitors of angiogenesis are designed to interfere with specific molecular targets on endothelial cells, it is attractive to consider imaging tests that are based on these molecular features. A growing list of molecularly targeted imaging agents is being developed

Table 2. Markers preferentially expressed on angiogenic and tumor blood vessels

Marker	Alternate names	Human	Mouse	Reference
Aminopeptidase A	APA, Glutamyl aminopeptidase; ENPEP; GP160		x	46
Aminopeptidase N	APN, CD13		x	46
Endoglin	CD105; ENG; TGF-β receptor complex component	x	x	84, 85
ED-B fibronectin	Extra-domain B or oncofetal domain fibronectin	x	x	12
Integrin $\alpha_v\beta_3$	Vitronectin receptor	x	x	49, 50, 51
Integrin $\alpha_v\beta_5$	Vitronectin receptor	x	x	19, 50
Integrin $\alpha_4\beta_1$	VLA4		x	86
α?Integrin $_5\beta_1$	Fibronectin receptor, VLA5	x	x	52, 53, 57
NG2 (on pericytes)	High-molecular weight melanoma associated antigen		x	46
Phosphatidylserine	PS		x	87
PDGFR-β associated molecule (on pericytes)			x	88
PV1	MECA32/PAL-E		x	89
ROBO4	Roundabout homolog-4	x	x	12
Delta-like ligand 4	Dll4; Delta-like 4; Delta-like 4 ligand		x	90, 91
Prostate-specific membrane antigen	PSMA	x		92
Tenascin-C		x	x	12
Tumor Endothelial Markers 1-8	TEM 1-8	x	x	43, 44, 93
VEGF/VEGF receptor complexes		x	x	94

to image angiogenesis. To date these agents have largely targeted integrins that are over-expressed on angiogenic vessels. However, due to the constraints of sensitivity, the current generation of targeted imaging agents is either PET or SPECT agents. By using advances in immunohistochemistry and scanning electron microscopy, it will be possible to determine the concentration and distribution of these molecular receptors and predict which imaging modalities are feasible as imaging agents.

5.1. Selective expression of molecules by tumor blood vessels

An essential property of angiogenesis inhibitors is their preferential effect on tumor vessels over normal blood vessels. Therefore, much effort in the development of angiogenesis inhibitors has focused on the identification of target molecules that are differentially or exclusively expressed on endothelial cells or other components of tumor blood vessels. In principle, agents that target molecules uniquely expressed on tumor vessels could be safely and effectively used alone or conjugated to toxins that destroy blood vessels. The agents could also be used to target contrast agents for clinical imaging and monitoring of anti-cancer therapy. In practice, however, manymolecular targets on tumor vessels are also found to some extent at sites of angiogenesis in wound healing or female reproductive organs and even on normal quiescent blood vessels.

The molecular expression of markers restricted to tumor vessels probably is not a prerequisite for drug efficacy. Molecules involved in VEGF signaling are widely distributed in normal organs, but inhibitors of this pathway have proven to be effective in preclinical tumor models and in human cancer (40, 41). Although VEGF receptors are present throughout the normal microvasculature, inhibitors of VEGF signaling cause significantly greater regression of tumor vessels than of normal capillaries (42). Multiple inhibitors of the VEGF pathway are already approved for clinical use and widely administered for treatment of human cancer.

The quest for selective targets on tumor vasculature continues, but no molecule truly specific to tumor vessels has been identified. Promising systematic search strategies have nonetheless emerged. Multiple novel human tumor endothelial markers (TEM) and corresponding mouse homologues have been identified by serial analysis of gene expression (SAGE) (43, 44). Other potential target molecules on blood vessels or extracellular matrix in tumors have been found by using *in vivo* phage display (45-48). Some of the molecular targets reportedly expressed preferentially at sites of angiogenesis in tumors or elsewhere are listed in Table 2.

Integrins are another well studied target on tumor blood vessels. The integrin family includes cell surface receptors for extracellular matrix components and receptors involved in leukocyte adhesion and migration. Multiple integrins, including $\alpha_v\beta_3$, $\alpha_v\beta_5$, $\alpha_4\beta_1$, and $\alpha_5\beta_1$, are upregulated on endothelial cells of blood vessels in at least some tumors (19, 49-53). The amount of upregulation of integrin $\alpha_5\beta_1$ increases with tumor progression (Figure 3A) (53).

Evidence that α_v integrins $\alpha_v\beta_3$ and $\alpha_v\beta_5$ play a key role in angiogenesis is a bit paradoxical because mice deficient in integrin subunits β_3 and/or β_5 have increased angiogenesis and tumor growth (54, 55). One explanation is that deletion of integrin β_3 or β_5 disrupts immune cell trafficking that helps drive tumor angiogenesis. Regardless of this issue, antibody and peptide inhibitors of integrins $\alpha_v\beta_3$ and $\alpha_5\beta_1$ are effective in mouse tumor models and are currently in clinical trials for cancer and other diseases (56).

Integrin $\alpha_5\beta_1$, which functions as a receptor for fibronectin, is expressed on the abluminal (basal) surface of endothelial cells in contact with fibronectin in the extracellular matrix. However, the integrin in tumors is also expressed on the luminal surface of endothelial cells, perhaps as a reflection of loss of cell polarity (53, 57). Because of this distribution, anti-integrin $\alpha_5\beta_1$ antibodies in the bloodstream have immediate access to the integrin on endothelial cells in tumors but not in normal vasculature (Figures 3A-C) (53, 57). Otherwise, circulating antibodies would have to extravasate to reach $\alpha_5\beta_1$ integrin on the abluminal surface. Although

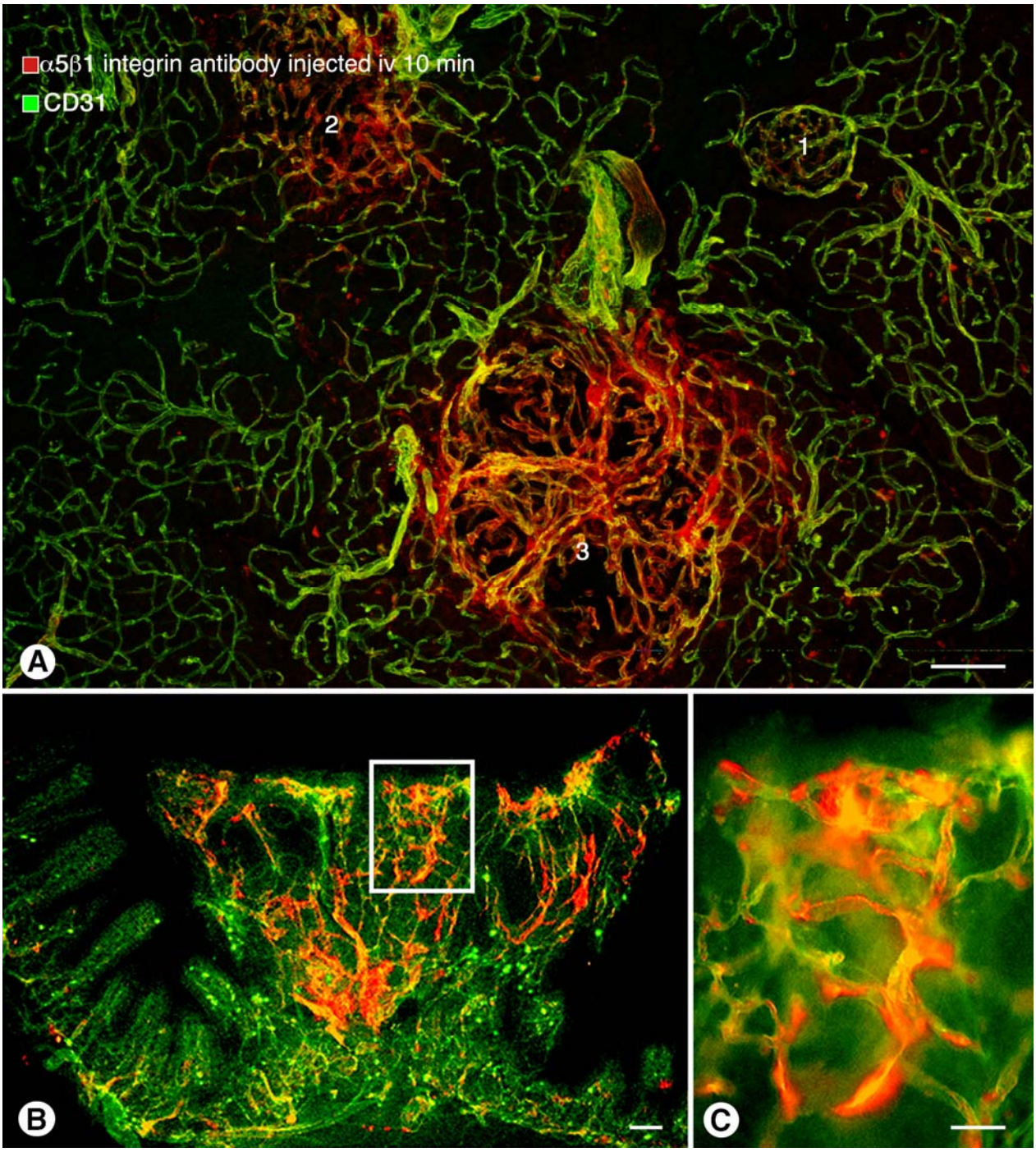

Figure 3. A. Confocal microscopic image of blood vessels (green, stained for CD31) in pancreas of untreated RIP-Tag2 transgenic mouse showing a relatively normal pancreatic islet (1) and two tumors (2, 3). Staining by anti-integrin $\alpha_5\beta_1$ antibody (red) injected intravenously 10 minutes before sacrifice is weak in the islet (1) but is strong in both tumors (2, 3). Little staining by the antibody is evident in the acinar pancreas. Bar: 100 µm. Reproduced with permission from (53) . B. Confocal microscopic image of blood vessels (green, stained for CD31) in intestine of adenomoatous polyposis coli (apc) mutant mouse. Anti-integrin $\alpha_5\beta_1$ antibody, which was injected intravenously 10 minutes before sacrifice, stained regions of $\alpha_5\beta_1$ integrin (red) in and around blood vessels of the adenoma but not in the adjacent normal intestine. Bar: 100 µm. Reproduced with permission from (53). C. Enlargement of boxed region in Figure 3B. Blood vessels in adenoma have fuzzy staining for anti-integrin $\alpha_5\beta_1$ antibody (red), suggestive of extravasated antibody binding to $\alpha_5\beta_1$ integrin on pericytes or other perivascular cells as well as on endothelial cells of tumor vessels. Bar: 50 µm. Reproduced with permission from (53).

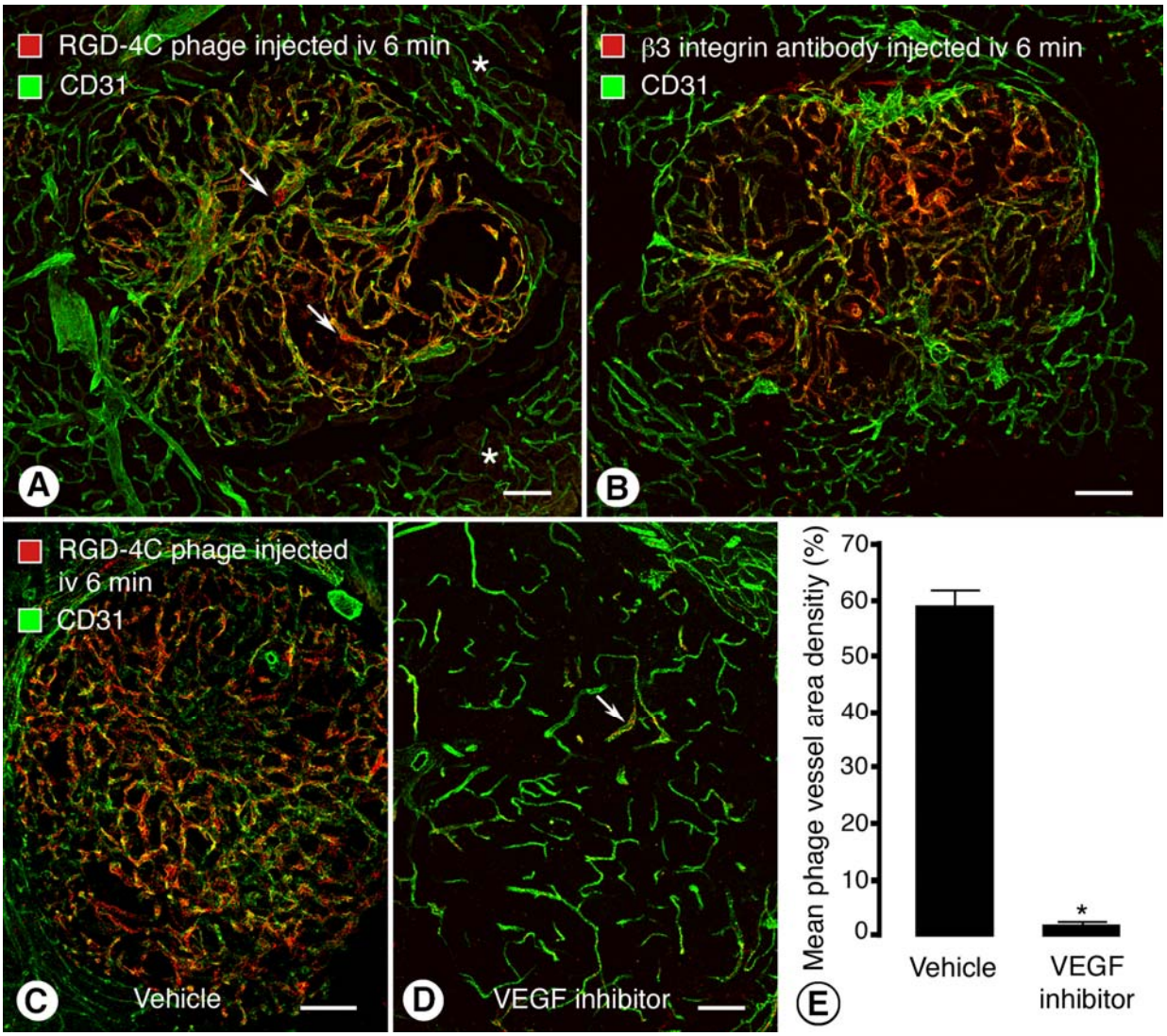

Figure 4. A. Localization of RGD-4C phage (red) mostly to blood vessels (green, stained for CD31) to RIP-Tag2 islet tumor and to a few small regions of extravasated phage (arrows). Acinar blood vessels (asterisks) do not contain RGD-4C phage. Bar: 50 µm. Reproduced with permission from (59). B. Luminal expression of β3 integrin in RIP-Tag2 tumor blood vessels. Confocal images show heterogenous expression of β3 integrin (CD61, red) in blood vessels (green, stained for CD31). Antibody to β3 integrin was injected intravenously before sacrifice. Bar: 50 µm. Reproduced with permission from (59). C-E. RGD-4C phage localization decreases in blood vessels after VEGF inhibition. Reproduced with permission from (59). C. RGD-4C phage (red) co-localizes extensively with tumor blood vessels (green, stained for CD31) in RIP-Tag2 mouse treated with vehicle for 7 days. Bar: 100 µm. D. A few surviving blood vessels (green) following VEGF inhibition for 7 days contain variable and lower amounts of RGD-4C phage (red, arrow) than vessels in vehicle-treated mice. Bar: 100 µm. E. Quantification of mean RGD-4C phage vessel area density in islet blood vessels of mice treated with vehicle or VEGF inhibitor for 7 days. (* = Significantly different, $P < 0001$).

tumor vessels are leaky to antibodies, extravasation does not occur uniformly in tumor vasculature (53, 57). Antibodies tend to extravasate and accumulate in patchy regions around tumor vessels and do not achieve a uniform distribution even after 24 hours (53, 57). The accessibility of the integrin on tumor vessels makes the integrin an attractive target for macromolecular diagnostics and therapeutics administered via the bloodstream.

Integrin $\alpha_5\beta_1$, like integrins $\alpha_v\beta_3$ and $\alpha_v\beta_5$, binds the arginine-glycine-aspartic (RGD) tripeptide sequence. Agents containing RGD peptides have thus been used to target tumor vessels (58). The selectivity of RGD targeting of tumor blood vessels has been confirmed by imaging the *in vivo* distribution of bacteriophage that are genetically engineered to express the cyclic peptide RGD-4C (59). RGD-4C phage selectively accumulate on tumor vessels known to express RGD-binding integrins on their luminal

surface, but not on adjacent normal blood vessels that lack the integrins (Figures 4A-B) (53, 57, 59).

Inhibition of VEGF signaling, which causes a rapid reduction in tumor vascularity, produces a profound reduction in expression of $\alpha_5\beta_1$ integrin on surviving tumor vessels (Figures 4C-E) (59). It is unclear whether this property will significantly impact the use of integrin targeted contrast agents to monitor anti-VEGF therapy of tumors (58).

5.2. Targeted angiogenesis imaging

A challenge to the molecular imaging of angiogenesis is that vessels comprise only a small percentage (less than 5%) of a tumor's mass so there are a relatively low number of targets in comparison to tumor cells, thus imaging needs to be very sensitive to detect low concentrations of the molecularly-targeted contrast agent (60). Because the number of targets is relatively small, currently only PET, SPECT and optical agents have sufficient sensitivity to be used in this manner. Despite limitations in their spatial resolution, PET and SPECT imaging are more likely to enter the clinic as targeted angiogenesis imaging methods than is MRI, indeed, clinical PET agents targeting the integrin $\alpha v\beta_3$ are already under development. Optical imaging is less likely to be used as a clinical modality because of the limited penetration of light in tissue, however, for the purposes of drug development, optical imaging in mice is more cost effective than the other modalities.

Since $\alpha v\beta_3$ integrin binds proteins displaying the triple amino acid sequence arginine-glycine-aspartic acid (RGD) it is a candidate for targeted imaging (61). RGD ligands linked to contrast agents, can potentially target the $\alpha_v\beta_3$ integrin. A number of carrier molecules can transport the RGD peptide to its target and enable delivery of a therapeutic payload, or contrast agent for imaging. For instance, viruses have been studied, notably adenovirus-RGD (62). Peptidomimetics are organic molecules that can mimic the short protein sequence RGD, to allow targeting of the $\alpha_v\beta_3$ integrin. Their small size means multiple peptidomimetics can be conjugated to a single carrier molecule, thus achieving a higher affinity, through binding several cell surface receptors simultaneously. Alternatively, integrin antagonists can be used for targeting. The integrin antagonist SU015 has been shown to preferentially bind to the $\alpha_v\beta_5$ and $\alpha v\beta_3$ integrins *in vitro* (63). Disintegrins are a class of low molecular weight, RGD- containing, cysteine-rich peptides isolated from the venom of various snakes (64). Echistatin is an example and has been shown to be an active inhibitor of both $\alpha_v\beta_3$ and $\alpha_5\beta_1$ integrins (65), offering another means of targeting imaging agents to these angiogenic markers. Greater specificity can be provided *via* monoclonal antibodies (mAb) directed at $\alpha_v\beta_3$ (66), however, the larger size of the mAb means higher background signal in the vessels and it may be difficult to distinguish specific from non-specific vascular activity. Sipkins *et al* employed MR to detect angiogenic 'hot spots' within rabbit tumors using LM609 mAb targeting of polymerized vesicles containing Gadolinium (67).

PET agents employing ^{18}F-labeled glycopeptides containing RGD sequences can be utilized to target angiogenic endothelial cells expressing the respective integrins (Figure 5A-B). Houston *et al* used a dual labeled peptide for PET and near infra-red optical imaging to investigate endothelial integrins (68). $\alpha v\beta_3$ integrin positive melanoma xenografts showed similar tumor-to-background ratios for both modalities, but a significantly higher signal-to-noise ratio with the optical images. Wu *et al* investigated ^{18}F-labeled tetrameric RGD peptide tracers in subcutaneous glioma xenografts (69). Micro-PET demonstrated significant uptake and good contrast within the tumors and specificity was proven by using a negative control to block $\alpha v\beta_3$ integrin receptors. The same group has recently demonstrated that a dimeric-RGD peptide labeled with a PET emitter can achieve a good linear relationship of signal to tissue integrin level (70). A variety of other PET imaging probes for imaging angiogenesis, and hence potentially anti-angiogenic effects, have been synthesized, including perfusion tracers such as ^{15}O-labeled water (71), and monoclonal antibodies against VEGF (72).

It should be noted that while PET or SPECT imaging offer the greatest potential for clinical translation of targeted angiogenesis imaging, the ability to target the $\alpha_v\beta_3$ integrin experimentally has also been demonstrated by US, MRI (Figure 5C-D), and optical imaging. Winter *et al,* for instance, have successfully demonstrated MR imaging of $\alpha v\beta_3$ integrins in areas of angiogenesis, using a perfluorocarbon emulsion nanoparticle containing Gd and targeting *via* peptidomimetics. They demonstrated a 126% increase in MR signal, pre-dominantly in the periphery of the tumor, but also in vessels proximal to the tumor in the VX-2 rabbit tumor model. Histology confirmed the presence of neo-angiogenesis within these areas. They have also used rabbit models of atherosclerosis, showing ~50% increase in MR signal in the angiogenic areas that surround the plaque, as confirmed by immunohistochemistry (73). This group used the same imaging methods for a murine model of melanoma. Contrast enhancement of angiogenesis within the tumors increased by 173% after targeted imaging. Mulder *et al* have produced liposomes with conjugated $\alpha_v\beta_3$-specific RGD peptides (74). The liposomes contained Gd and fluorescein-PE, making them amenable to MR and fluorescence imaging. MR demonstrated increased enhancement in areas of angiogenesis, whilst *ex vivo* fluorescent microscopy confirmed binding of the liposomes to the activated tumor epithelium. Ellegala *et al* have used contrast enhanced US to image microbubbles targeted to endothelial $\alpha v\beta_3$ integrin (75). Using RGD-bearing echistatin conjugates for targeting, they imaged murine glioma xenografts at 14 and 28 days post implantation. Microbubble adhesion was established by *in vivo* confocal microscopy. Immunohistochemistry was used to confirm the expression of $\alpha v\beta_3$ integrin in these areas. US may also be used to increase targeting efficiency. Application of acoustic energy as an US pulse has been shown *in vitro* to increase

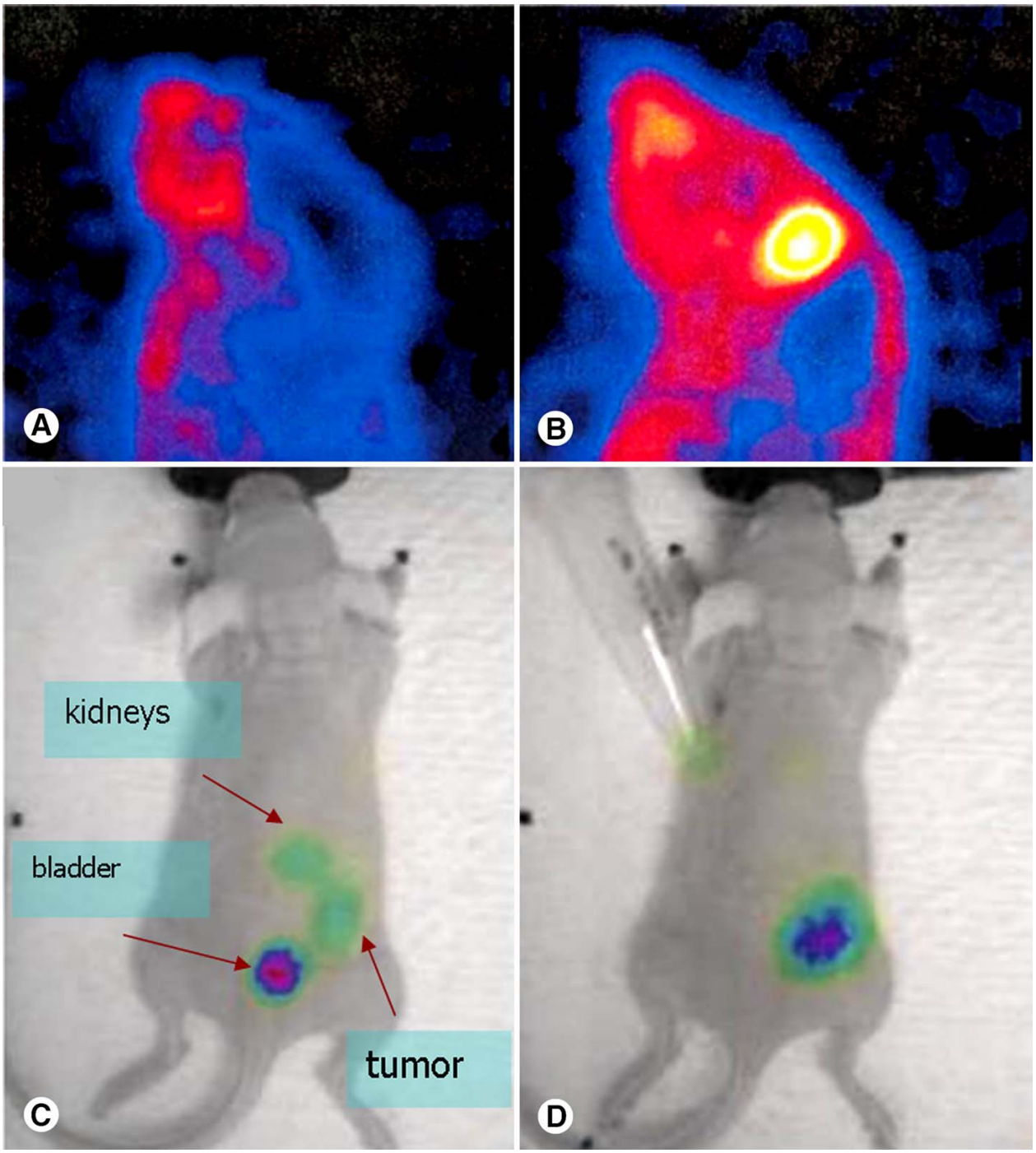

Figures 5. A-B. MicroPET imaging following 200 mCi tail vein injection of (^{18}F)-FB-RGD into (A) normal mouse and (B) U25IT glioblastoma-bearing nude mouse, at 30 min. Note increased uptake in the tumor-bearing mouse. Reproduced with permission from Chen X et al. (80). Image reproduced with permission from Dr P. S. Conti (University of Southern California, USA), by permission of Nuclear Medicine and Biology. C-D. ^{111}Indium-RGD scintigraphy scan superimposed on white light image of a mouse bearing M21 melanoma xenograft. (C) Increased uptake is seen in the tumor, kidneys and bladder. (D) Delayed image shows that the uptake has cleared the kidneys and bladder and is mostly in the tumor. Images courtesy of Andy Boswell, and Celeste Regino, NCI, Bethesda, MD.

the adhesion of microbubbles to the endothelium as much as 20 fold when they are targeted to $\alpha v\beta_3$ (76). Targeted optical imaging has also been used to image $\alpha v\beta_3$. Cheng *et al* evaluated Cy5.5-conjugated mono-, di-, and tetrameric RGD peptides in a subcutaneous glioblastoma xenograft model in order to investigate the effect of multimerization

of RGD peptide on integrin avidity and tumor targeting efficacy (77). They reported that the multimerization of RGD peptide on Cy5.5 results in moderate improvement of imaging characteristics of the tetramer, compared to that of the monomer and dimeric counterparts. Aina *et al* synthesized a new peptide called "OA02" and labeled with near-infrared probes, that binds to alpha3 integrin subunit on ovarian adenocarcinoma cells. After intravenous injection of OA02 in ovarian tumor-bearing mice it displayed highly specific tumor uptake within 15 minutes which persisted for 70 minutes (78). Significant barriers related to sensitivity with MRI and depth penetration with optical imaging need to be overcome before clinical translation is possible for these imaging modalities.

6. ACKNOWLEDGEMENTS

This research was supported by the Intramural Research Program of the NIH, National Cancer Institute, Center for Cancer Research to PLC. Additionally, this work was supported in part by National Institutes of Health grants HL24136 and HL59157 from the National Heart, Lung, and Blood Institute and CA82923 from the National Cancer Institute to DMcD. The authors have no conflicting financial interests.

7. REFERENCES

1. Barentsz, J. O., O. Berger-Hartog, J. A. Witjes, C. Hulsbergen-van der Kaa, G. O. Oosterhof, J. A. VanderLaak, H. Kondacki & S. H. Ruijs: Evaluation of chemotherapy in advanced urinary bladder cancer with fast dynamic contrast-enhanced MR imaging. *Radiology*, 207, 791-7 (1998)

2. Esserman, L., N. Hylton, T. George & N. Weidner: Contrast-Enhanced Magnetic Resonance Imaging to Assess Tumor Histopathology and Angiogenesis in Breast Carcinoma. *Breast J*, 5, 13-21 (1999)

3. Hulka, C. A., W. B. Edmister, B. L. Smith, L. Tan, D. C. Sgroi, T. Campbell, D. B. Kopans & R. M. Weisskoff: Dynamic echo-planar imaging of the breast: experience in diagnosing breast carcinoma and correlation with tumor angiogenesis. *Radiology*, 205, 837-42 (1997)

4. Kuhl, C. K., P. Mielcareck, S. Klaschik, C. Leutner, E. Wardelmann, J. Gieseke & H. H. Schild: Dynamic breast MR imaging: are signal intensity time course data useful for differential diagnosis of enhancing lesions? *Radiology*, 211, 101-10 (1999)

5. Baluk, P., H. Hashizume & D. M. McDonald: Cellular abnormalities of blood vessels as targets in cancer. *Curr Opin Genet Dev*, 15, 102-11 (2005)

6. Hashizume, H., P. Baluk, S. Morikawa, J. W. McLean, G. Thurston, S. Roberge, R. K. Jain & D. M. McDonald: Openings between defective endothelial cells explain tumor vessel leakiness. *Am J Pathol*, 156, 1363-80 (2000)

7. Nakahara, T., S. M. Norberg, D. R. Shalinsky, D. D. Hu-Lowe & D. M. McDonald: Effect of inhibition of vascular endothelial growth factor signaling on distribution of extravasated antibodies in tumors. *Cancer Res*, 66, 1434-45 (2006)

8. Inai, T., M. Mancuso, H. Hashizume, F. Baffert, A. Haskell, P. Baluk, D. D. Hu-Lowe, D. R. Shalinsky, G. Thurston, G. D. Yancopoulos & D. M. McDonald: Inhibition of vascular endothelial growth factor (VEGF) signaling in cancer causes loss of endothelial fenestrations, regression of tumor vessels, and appearance of basement membrane ghosts. *Am J Pathol*, 165, 35-52 (2004)

9. Baluk, P., S. Morikawa, A. Haskell, M. Mancuso & D. M. McDonald: Abnormalities of basement membrane on blood vessels and endothelial sprouts in tumors. *Am J Pathol*, 163, 1801-15 (2003)

10. Armulik, A., A. Abramsson & C. Betsholtz: Endothelial/pericyte interactions. *Circ Res*, 97, 512-23 (2005)

11. Kalluri, R.: Basement membranes: structure, assembly and role in tumour angiogenesis. *Nat Rev Cancer*, 3, 422-33 (2003)

12. Neri, D. & R. Bicknell: Tumour vascular targeting. *Nat Rev Cancer*, 5, 436-46 (2005)

13. de Visser, K. E., A. Eichten & L. M. Coussens: Paradoxical roles of the immune system during cancer development. *Nat Rev Cancer*, 6, 24-37 (2006)

14. Kalluri, R. & M. Zeisberg: Fibroblasts in cancer. *Nat Rev Cancer*, 6, 392-401 (2006)

15. Hobbs, S. K., W. L. Monsky, F. Yuan, W. G. Roberts, L. Griffith, V. P. Torchilin & R. K. Jain: Regulation of transport pathways in tumor vessels: role of tumor type and microenvironment. *Proc Natl Acad Sci U S A*, 95, 4607-12 (1998)

16. Kohn, S., J. A. Nagy, H. F. Dvorak & A. M. Dvorak: Pathways of macromolecular tracer transport across venules and small veins. Structural basis for the hyperpermeability of tumor blood vessels. *Lab Invest*, 67, 596-607 (1992)

17. Michel, C. C. & F. E. Curry: Microvascular permeability. *Physiol Rev*, 79, 703-61 (1999)

18. Padera, T. P., A. Kadambi, E. di Tomaso, C. M. Carreira, E. B. Brown, Y. Boucher, N. C. Choi, D. Mathisen, J. Wain, E. J. Mark, L. L. Munn & R. K. Jain: Lymphatic metastasis in the absence of functional intratumor lymphatics. *Science*, 296, 1883-6 (2002)

19. Ruoslahti, E.: Specialization of tumour vasculature. *Nat Rev Cancer*, 2, 83-90 (2002)

20. Jain, R. K.: Normalization of tumor vasculature: an emerging concept in antiangiogenic therapy. *Science*, 307, 58-62 (2005)

21. McDonald, D. M. & P. L. Choyke: Imaging of angiogenesis: from microscope to clinic. *Nat Med*, 9, 713-25 (2003)

22. Willett, C. G., Y. Boucher, E. di Tomaso, D. G. Duda, L. L. Munn, R. T. Tong, D. C. Chung, D. V. Sahani, S. P. Kalva, S. V. Kozin, M. Mino, K. S. Cohen, D. T. Scadden, A. C. Hartford, A. J. Fischman, J. W. Clark, D. P. Ryan, A. X. Zhu, L. S. Blaszkowsky, H. X. Chen, P. C. Shellito, G. Y. Lauwers & R. K. Jain: Direct evidence that the VEGF-specific antibody bevacizumab has antivascular effects in human rectal cancer. *Nat Med*, 10, 145-7 (2004)

23. Padhani, A. R. & M. O. Leach: Antivascular cancer treatments: functional assessments by dynamic contrast-enhanced magnetic resonance imaging. *Abdom Imaging*, 30, 324-41 (2005)

24. Tofts, P. S., G. Brix, D. L. Buckley, J. L. Evelhoch, E. Henderson, M. V. Knopp, H. B. Larsson, T. Y. Lee, N. A. Mayr, G. J. Parker, R. E. Port, J. Taylor & R. M.

Weisskoff: Estimating kinetic parameters from dynamic contrast-enhanced T (1)-weighted MRI of a diffusable tracer: standardized quantities and symbols. *J Magn Reson Imaging*, 10, 223-32 (1999)
25. Choyke, P. L., A. J. Dwyer & M. V. Knopp: Functional tumor imaging with dynamic contrast-enhanced magnetic resonance imaging. *J Magn Reson Imaging*, 17, 509-20 (2003)
26. Brix, G., W. Semmler, R. Port, L. R. Schad, G. Layer & W. J. Lorenz: Pharmacokinetic parameters in CNS Gd-DTPA enhanced MR imaging. *J Comput Assist Tomogr*, 15, 621-8 (1991)
27. Furman-Haran, E., R. Margalit, D. Grobgeld & H. Degani: Dynamic contrast-enhanced magnetic resonance imaging reveals stress-induced angiogenesis in MCF7 human breast tumors. *Proc Natl Acad Sci U S A*, 93, 6247-51 (1996)
28. Knopp, M. V., F. L. Giesel, H. Marcos, H. von Tengg-Kobligk & P. Choyke: Dynamic contrast-enhanced magnetic resonance imaging in oncology. *Top Magn Reson Imaging*, 12, 301-8 (2001)
29. Marzola, P., A. Degrassi, L. Calderan, P. Farace, C. Crescimanno, E. Nicolato, A. Giusti, E. Pesenti, A. Terron, A. Sbarbati, T. Abrams, L. Murray & F. Osculati: In vivo assessment of antiangiogenic activity of SU6668 in an experimental colon carcinoma model. *Clin Cancer Res*, 10, 739-50 (2004)
30. Lee, L., S. Sharma, B. Morgan, P. Allegrini, C. Schnell, J. Brueggen, R. Cozens, M. Horsfield, C. Guenther, W. P. Steward, J. Drevs, D. Lebwohl, J. Wood & P. M. McSheehy: Biomarkers for assessment of pharmacologic activity for a vascular endothelial growth factor (VEGF) receptor inhibitor, PTK787/ZK 222584 (PTK/ZK): translation of biological activity in a mouse melanoma metastasis model to phase I studies in patients with advanced colorectal cancer with liver metastases. *Cancer Chemother Pharmacol*, 57, 761-71 (2006)
31. de Lussanet, Q. G., R. G. Beets-Tan, W. H. Backes, D. W. van der Schaft, J. M. van Engelshoven, K. H. Mayo & A. W. Griffioen: Dynamic contrast-enhanced magnetic resonance imaging at 1.5 Tesla with gadopentetate dimeglumine to assess the angiostatic effects of anginex in mice. *Eur J Cancer*, 40, 1262-8 (2004)
32. Morgan, B., A. L. Thomas, J. Drevs, J. Hennig, M. Buchert, A. Jivan, M. A. Horsfield, K. Mross, H. A. Ball, L. Lee, W. Mietlowski, S. Fuxuis, C. Unger, K. O'Byrne, A. Henry, G. R. Cherryman, D. Laurent, M. Dugan, D. Marme & W. P. Steward: Dynamic contrast-enhanced magnetic resonance imaging as a biomarker for the pharmacological response of PTK787/ZK 222584, an inhibitor of the vascular endothelial growth factor receptor tyrosine kinases, in patients with advanced colorectal cancer and liver metastases: results from two phase I studies. *J Clin Oncol*, 21, 3955-64 (2003)
33. Liu, G., H. S. Rugo, G. Wilding, T. M. McShane, J. L. Evelhoch, C. Ng, E. Jackson, F. Kelcz, B. M. Yeh, F. T. Lee, Jr., C. Charnsangavej, J. W. Park, E. A. Ashton, H. M. Steinfeldt, Y. K. Pithavala, S. D. Reich & R. S. Herbst: Dynamic contrast-enhanced magnetic resonance imaging as a pharmacodynamic measure of response after acute dosing of AG-013736, an oral angiogenesis inhibitor, in patients with advanced solid tumors: results from a phase I study. *J Clin Oncol*, 23, 5464-73 (2005)
34. Wedam, S. B., J. A. Low, S. X. Yang, C. K. Chow, P. Choyke, D. Danforth, S. M. Hewitt, A. Berman, S. M. Steinberg, D. J. Liewehr, J. Plehn, A. Doshi, D. Thomasson, N. McCarthy, H. Koeppen, M. Sherman, J. Zujewski, K. Camphausen, H. Chen & S. M. Swain: Antiangiogenic and antitumor effects of bevacizumab in patients with inflammatory and locally advanced breast cancer. *J Clin Oncol*, 24, 769-77 (2006)
35. Xiong, H. Q., R. Herbst, S. C. Faria, C. Scholz, D. Davis, E. F. Jackson, T. Madden, D. McConkey, M. Hicks, K. Hess, C. A. Charnsangavej & J. L. Abbruzzese: A phase I surrogate endpoint study of SU6668 in patients with solid tumors. *Invest New Drugs*, 22, 459-66 (2004)
36. Huang, X., M. K. Wong, H. Yi, S. Watkins, A. D. Laird, S. F. Wolf & E. Gorelik: Combined therapy of local and metastatic 4T1 breast tumor in mice using SU6668, an inhibitor of angiogenic receptor tyrosine kinases, and the immunostimulator B7.2-IgG fusion protein. *Cancer Res*, 62, 5727-35 (2002)
37. Ning, S., D. Laird, J. M. Cherrington & S. J. Knox: The antiangiogenic agents SU5416 and SU6668 increase the antitumor effects of fractionated irradiation. *Radiat Res*, 157, 45-51 (2002)
38. Medved, M., G. Karczmar, C. Yang, J. Dignam, T. F. Gajewski, H. Kindler, E. Vokes, P. MacEneany, M. T. Mitchell & W. M. Stadler: Semiquantitative analysis of dynamic contrast enhanced MRI in cancer patients: Variability and changes in tumor tissue over time. *J Magn Reson Imaging*, 20, 122-8 (2004)
39. Preda, A., M. van Vliet, G. P. Krestin, R. C. Brasch & C. F. van Dijke: Magnetic resonance macromolecular agents for monitoring tumor microvessels and angiogenesis inhibition. *Invest Radiol*, 41, 325-31 (2006)
40. Kowanetz, M. & N. Ferrara: Vascular endothelial growth factor signaling pathways: therapeutic perspective. Clin *Cancer Res*, 12, 5018-22 (2006)
41. Olsson, A. K., A. Dimberg, J. Kreuger & L. Claesson-Welsh: VEGF receptor signalling - in control of vascular function. *Nat Rev Mol Cell Biol*, 7, 359-71 (2006)
42. Kamba, T., B. Y. Tam, H. Hashizume, A. Haskell, B. Sennino, M. R. Mancuso, S. M. Norberg, S. M. O'Brien, R. B. Davis, L. C. Gowen, K. D. Anderson, G. Thurston, S. Joho, M. L. Springer, C. J. Kuo & D. M. McDonald: VEGF-dependent plasticity of fenestrated capillaries in the normal adult microvasculature. *Am J Physiol Heart Circ Physiol*, 290, H560-76 (2006)
43. Nanda, A. & B. St Croix: Tumor endothelial markers: new targets for cancer therapy. *Curr Opin Oncol*, 16, 44-9 (2004)
44. St Croix, B., C. Rago, V. Velculescu, G. Traverso, K. E. Romans, E. Montgomery, A. Lal, G. J. Riggins, C. Lengauer, B. Vogelstein & K. W. Kinzler: Genes expressed in human tumor endothelium. *Science*, 289, 1197-202 (2000)
45. Arap, W., M. G. Kolonin, M. Trepel, J. Lahdenranta, M. Cardo-Vila, R. J. Giordano, P. J. Mintz, P. U. Ardelt, V. J. Yao, C. I. Vidal, L. Chen, A. Flamm, H. Valtanen, L. M. Weavind, M. E. Hicks, R. E. Pollock, G. H. Botz, C. D. Bucana, E. Koivunen, D. Cahill, P. Troncoso, K. A. Baggerly, R. D. Pentz, K. A. Do, C. J. Logothetis & R.

Pasqualini: Steps toward mapping the human vasculature by phage display. *Nat Med*, 8, 121-7 (2002)
46. Hajitou, A., R. Pasqualini & W. Arap: Vascular targeting: recent advances and therapeutic perspectives. Trends *Cardiovasc Med*, 16, 80-8 (2006)
47. Pilch, J., D. M. Brown, M. Komatsu, T. A. Jarvinen, M. Yang, D. Peters, R. M. Hoffman & E. Ruoslahti: Peptides selected for binding to clotted plasma accumulate in tumor stroma and wounds. *Proc Natl Acad Sci U S A*, 103, 2800-4 (2006)
48. Ruoslahti, E.: Vascular zip codes in angiogenesis and metastasis. *Biochem Soc Trans*, 32, 397-402 (2004)
49. Brooks, P. C., S. Stromblad, R. Klemke, D. Visscher, F. H. Sarkar & D. A. Cheresh: Antiintegrin alpha v beta 3 blocks human breast cancer growth and angiogenesis in human skin. *J Clin Invest*, 96, 1815-22 (1995)
50. Eliceiri, B. P. & D. A. Cheresh: Role of alpha v integrins during angiogenesis. *Cancer J*, 6 Suppl 3, S245-9 (2000)
51. Hood, J. D. & D. A. Cheresh: Role of integrins in cell invasion and migration. *Nat Rev Cancer*, 2, 91-100 (2002)
52. Kim, S., K. Bell, S. A. Mousa & J. A. Varner: Regulation of angiogenesis in vivo by ligation of integrin alpha5beta1 with the central cell-binding domain of fibronectin. *Am J Pathol*, 156, 1345-62 (2000)
53.Parsons-Wingerter, P., I. M. Kasman, S. Norberg, A. Magnussen, S. Zanivan, A. Rissone, P. Baluk, C. J. Favre, U. Jeffry, R. Murray & D. M. McDonald: Uniform overexpression and rapid accessibility of alpha5beta1 integrin on blood vessels in tumors. *Am J Pathol*, 167, 193-211 (2005)
54. Hynes, R. O.: A reevaluation of integrins as regulators of angiogenesis. *Nat Med*, 8, 918-21 (2002)
55. Taverna, D., H. Moher, D. Crowley, L. Borsig, A. Varki & R. O. Hynes: Increased primary tumor growth in mice null for beta3- or beta3/beta5-integrins or selectins. *Proc Natl Acad Sci U S A*, 101, 763-8 (2004)
56. Jin, H. & J. Varner: Integrins: roles in cancer development and as treatment targets. *Br J Cancer*, 90, 561-5 (2004)
57. Magnussen, A., I. M. Kasman, S. Norberg, P. Baluk, R. Murray & D. M. McDonald: Rapid access of antibodies to alpha5beta1 integrin overexpressed on the luminal surface of tumor blood vessels. *Cancer Res*, 65, 2712-21 (2005)
58. Meyer, A., J. Auernheimer, A. Modlinger & H. Kessler: Targeting RGD recognizing integrins: drug development, biomaterial research, tumor imaging and targeting. *Curr Pharm Des*, 12, 2723-47 (2006)
59. Yao, V. J., M. G. Ozawa, A. S. Varner, I. M. Kasman, Y. H. Chanthery, R. Pasqualini, W. Arap & D. M. McDonald: Antiangiogenic therapy decreases integrin expression in normalized tumor blood vessels. *Cancer Res*, 66, 2639-49 (2006)
60. Miller, J. C., H. H. Pien, D. Sahani, A. G. Sorensen & J. H. Thrall: Imaging angiogenesis: applications and potential for drug development. *J Natl Cancer Inst*, 97, 172-87 (2005)
61. Ruoslahti, E. & M. D. Pierschbacher: Arg-Gly-Asp: a versatile cell recognition signal. *Cell*, 44, 517-8 (1986)
62. Xiong, Z., Z. Cheng, X. Zhang, M. Patel, J. C. Wu, S. S. Gambhir & X. Chen: Imaging Chemically Modified Adenovirus for Targeting Tumors Expressing Integrin {alpha}v{beta}3 in Living Mice with Mutant Herpes Simplex Virus Type 1 Thymidine Kinase PET Reporter Gene. *J Nucl Med*, 47, 130-139 (2006)
63. Mousa, S. A.: Alpha v integrin affinity/specificity and antiangiogenesis effect of a novel tetraaza cyclic peptide derivative, SU015, in various species. *J Cardiovasc Pharmacol*, 45, 462-7 (2005)
64. Gould, R. J., M. A. Polokoff, P. A. Friedman, T. F. Huang, J. C. Holt, J. J. Cook & S. Niewiarowski: Disintegrins: a family of integrin inhibitory proteins from viper venoms. *Proc Soc Exp Biol Med*, 195, 168-71 (1990)
65. Pfaff, M., M. A. McLane, L. Beviglia, S. Niewiarowski & R. Timpl: Comparison of disintegrins with limited variation in the RGD loop in their binding to purified integrins alpha IIb beta 3, alpha V beta 3 and alpha 5 beta 1 and in cell adhesion inhibition. *Cell Adhes Commun*, 2, 491-501 (1994)
66. Charo, I. F., L. Nannizzi, J. W. Smith & D. A. Cheresh: The vitronectin receptor alpha v beta 3 binds fibronectin and acts in concert with alpha 5 beta 1 in promoting cellular attachment and spreading on fibronectin. *J Cell Biol*, 111, 2795-800 (1990)
67. Sipkins, D. A., D. A. Cheresh, M. R. Kazemi, L. M. Nevin, M. D. Bednarski & K. C. Li: Detection of tumor angiogenesis in vivo by alphaVbeta3-targeted magnetic resonance imaging. *Nat Med*, 4, 623-6 (1998)
68. Houston, J. P., S. Ke, W. Wang, C. Li & E. M. Sevick-Muraca: Quality analysis of in vivo near-infrared fluorescence and conventional gamma images acquired using a dual-labeled tumor-targeting probe. *J Biomed Opt*, 10, 054010 (2005)
69. Wu, Y., X. Zhang, Z. Xiong, Z. Cheng, D. R. Fisher, S. Liu, S. S. Gambhir & X. Chen: microPET imaging of glioma integrin {alpha}v{beta}3 expression using (64)Cu-labeled tetrameric RGD peptide. *J Nucl Med*, 46, 1707-18 (2005)
70. Zhang, X., Z. Xiong, Y. Wu, W. Cai, J. R. Tseng, S. S. Gambhir & X. Chen: Quantitative PET Imaging of Tumor Integrin {alpha}v{beta}3 Expression with 18F-FRGD2. *J Nucl Med*, 47, 113-21 (2006)
71. Wilson, C. B., A. A. Lammertsma, C. G. McKenzie, K. Sikora & T. Jones: Measurements of blood flow and exchanging water space in breast tumors using positron emission tomography: a rapid and noninvasive dynamic method. *Cancer Res*, 52, 1592-7 (1992)
72. Collingridge, D. R., V. A. Carroll, M. Glaser, E. O. Aboagye, S. Osman, O. C. Hutchinson, H. Barthel, S. K. Luthra, F. Brady, R. Bicknell, P. Price & A. L. Harris: The development of [(124)I]iodinated-VG76e: a novel tracer for imaging vascular endothelial growth factor in vivo using positron emission tomography. *Cancer Res*, 62, 5912-9 (2002)
73. Winter, P. M., S. D. Caruthers, A. Kassner, T. D. Harris, L. K. Chinen, J. S. Allen, E. K. Lacy, H. Zhang, J. D. Robertson, S. A. Wickline & G. M. Lanza: Molecular imaging of angiogenesis in nascent Vx-2 rabbit tumors using a novel alpha (nu)beta3-targeted nanoparticle and 1.5 tesla magnetic resonance imaging. *Cancer Res*, 63, 5838-43 (2003)
74. Mulder, W. J., G. J. Strijkers, J. W. Habets, E. J. Bleeker, D. W. van der Schaft, G. Storm, G. A. Koning, A. W. Griffioen & K. Nicolay: MR molecular imaging and

fluorescence microscopy for identification of activated tumor endothelium using a bimodal lipidic nanoparticle. *Faseb J*, 19, 2008-10 (2005)
75. Ellegala, D. B., H. Leong-Poi, J. E. Carpenter, A. L. Klibanov, S. Kaul, M. E. Shaffrey, J. Sklenar & J. R. Lindner: Imaging tumor angiogenesis with contrast ultrasound and microbubbles targeted to alpha (v)beta3. *Circulation*, 108, 336-41 (2003)
76. Zhao, S., M. Borden, S. H. Bloch, D. Kruse, K. W. Ferrara & P. A. Dayton: Radiation-force assisted targeting facilitates ultrasonic molecular imaging. *Mol Imaging*, 3, 135-48 (2004)
77. Cheng, Z., Y. Wu, Z. Xiong, S. S. Gambhir & X. Chen: Near-infrared fluorescent RGD peptides for optical imaging of integrin alphavbeta3 expression in living mice. *Bioconjug Chem*, 16, 1433-41 (2005)
78. Aina, O. H., J. Marik, R. Gandour-Edwards & K. S. Lam: Near-infrared optical imaging of ovarian cancer xenografts with novel alpha 3-integrin binding peptide "OA02". *Mol Imaging*, 4, 439-47 (2005)
79. Baluk. P., C. G. Lee, H. Link, E. Ator, A. Haskell, J. A. Elias, D. M. McDonald: Regulated angiogenesis and vascular regression in mice overexpressing vascular endothelial growth factor in airways. *Am J Pathol*, 165,1071-85 (2004)
80. Chen, X., R. Park, A. H. Shahinian, M. Tohme, V. Khankaldyyan, M. H. Bozorgzadeh, J. R. Bading, R. Moats, W. E. Laug & P. S. Conti: 18F-labeled RGD peptide: initial evaluation for imaging brain tumor angiogenesis. *Nucl Med Biol*, 31, 179-89(2004)
81. Mross, K., J. Drevs, M. Muller, M. Medinger, D. Marme, J. Hennig, B. Morgan, D. Lebwohl, E. Masson, Y. Y. Ho, C. Gunther, D. Laurent & C. Unger: Phase I clinical and pharmacokinetic study of PTK/ZK, a multiple VEGF receptor inhibitor, in patients with liver metastases from solid tumours. *Eur J Cancer*, 41, 1291-9(2005)
82. Thomas, A. L., B. Morgan, M. A. Horsfield, A. Higginson, A. Kay, L. Lee, E. Masson, M. Puccio-Pick, D. Laurent & W. P. Steward: Phase I study of the safety, tolerability, pharmacokinetics, and pharmacodynamics of PTK787/ZK 222584 administered twice daily in patients with advanced cancer. *J Clin Oncol*, 23, 4162-71(2005)
83. Galbraith, S. M., R. J. Maxwell, M. A. Lodge, G. M. Tozer, J. Wilson, N. J. Taylor, J. J. Stirling, L. Sena, A. R. Padhani & G. J. Rustin: Combretastatin A4 phosphate has tumor antivascular activity in rat and man as demonstrated by dynamic magnetic resonance imaging. *J Clin Oncol*, 21, 2831-42(2003)
84. Burrows, F. J., E. J. Derbyshire, P. L. Tazzari, P. Amlot, A. F. Gazdar, S. W. King, M. Letarte, E. S. Vitetta & P. E. Thorpe: Up-regulation of endoglin on vascular endothelial cells in human solid tumors: implications for diagnosis and therapy. *Clin Cancer Res*, 1, 1623-34(1995)
85. Takahashi, N., A. Haba, F. Matsuno & B. K. Seon: Antiangiogenic therapy of established tumors in human skin/severe combined immunodeficiency mouse chimeras by anti-endoglin (CD105) monoclonal antibodies, and synergy between anti-endoglin antibody and cyclophosphamide. *Cancer Res*, 61, 7846-54(2001)
86. Jin, H., J. Su, B. Garmy-Susini, J. Kleeman & J. Varner: Integrin alpha4beta1 promotes monocyte trafficking and angiogenesis in tumors. *Cancer Res*, 66, 2146-52(2006)
87. Huang, X., M. Bennett & P. E. Thorpe: A monoclonal antibody that binds anionic phospholipids on tumor blood vessels enhances the antitumor effect of docetaxel on human breast tumors in mice. *Cancer Res*, 65, 4408-16(2005)
88. Joyce, J. A., P. Laakkonen, M. Bernasconi, G. Bergers, E. Ruoslahti & D. Hanahan: Stage-specific vascular markers revealed by phage display in a mouse model of pancreatic islet tumorigenesis. *Cancer Cell*, 4, 393-403(2003)
89. Madden, S. L., B. P. Cook, M. Nacht, W. D. Weber, M. R. Callahan, Y. Jiang, M. R. Dufault, X. Zhang, W. Zhang, J. Walter-Yohrling, C. Rouleau, V. R. Akmaev, C. J. Wang, X. Cao, T. B. St Martin, B. L. Roberts, B. A. Teicher, K. W. Klinger, R. V. Stan, B. Lucey, E. B. Carson-Walter, J. Laterra & K. A. Walter: Vascular gene expression in nonneoplastic and malignant brain. *Am J Pathol*, 165, 601-8(2004)
90. Ridgway, J., G. Zhang, Y. Wu, S. Stawicki, W. C. Liang, Y. Chanthery, J. Kowalski, R. J. Watts, C. Callahan, I. Kasman, M. Singh, M. Chien, C. Tan, J. A. Hongo, F. de Sauvage, G. Plowman & M. Yan: Inhibition of Dll4 signalling inhibits tumour growth by deregulating angiogenesis. *Nature*, 444, 1083-7(2006)
91. Noguera-Troise, I., C. Daly, N. J. Papadopoulos, S. Coetzee, P. Boland, N. W. Gale, H. C. Lin, G. D. Yancopoulos & G. Thurston: Blockade of Dll4 inhibits tumour growth by promoting non-productive angiogenesis. *Nature*, 444, 1032-7(2006)
92. Chang, S. S., D. S. O'Keefe, D. J. Bacich, V. E. Reuter, W. D. Heston & P. B. Gaudin: Prostate-specific membrane antigen is produced in tumor-associated neovasculature. *Clin Cancer Res*, 5, 2674-81(1999)
93. Beaty, R. M., J. B. Edwards, K. Boon, I. M. Siu, J. E. Conway & G. J. Riggins: PLXDC1 (TEM7) is identified in a genome-wide expression screen of glioblastoma endothelium. *J Neurooncol* (2006)
94. Brekken, R. A., X. Huang, S. W. King & P. E. Thorpe: Vascular endothelial growth factor as a marker of tumor endothelium. *Cancer Res*, 58, 1952-9(1998)

Key Words: Angiogenesis, Tumor neovasculature, Integrins, Endothelial cell, DCE-MRI, PET, SPECT, Review

Send correspondence to: Peter L. Choyke, M.D., Molecular Imaging Program, National Institutes of Health, Bethesda, MD 20892-1182, Tel: 301-451-6039, Fax 301-496-9933, E-mail: pchoyke@nih.gov

http://www.bioscience.org/current/vol12.htm